Marine Life Science & Technology (2024) 6:102–114
https://doi.org/10.1007/s42995-023-00210-0

RESEARCH PAPER

Griseofulvin enantiomers and bromine-containing griseofulvin derivatives with antifungal activity produced by the mangrove endophytic fungus *Nigrospora* sp. QQYB1

Ge Zou[1] · Wencong Yang[1] · Tao Chen[1] · Zhaoming Liu[1,2] · Yan Chen[1,3] · Taobo Li[1] · Gulab Said[4] · Bing Sun[1] · Bo Wang[1] · Zhigang She[1]

Received: 9 April 2023 / Accepted: 8 October 2023 / Published online: 4 December 2023

Abstract

Marine microorganisms have long been recognized as potential sources for drug discovery. Griseofulvin was one of the first antifungal natural products and has been used as an antifungal agent for decades. In this study, 12 new griseofulvin derivatives [(±)-**1**−**2**, (+)-**3**, (±)-**4**, **10**−**12**, and **14**−**15**] and two new griseofulvin natural products (**9** and **16**) together with six known analogues [(−)-**3**, **5**−**8**, and **13**] were isolated from the mangrove-derived fungus *Nigrospora* sp. QQYB1 treated with 0.3% NaCl or 2% NaBr in rice solid medium. Their 2D structures and absolute configurations were established by extensive spectroscopic analysis (1D and 2D NMR, HRESIMS), ECD spectra, computational calculation, DP4 + analysis, and X-ray single-crystal diffraction. Compounds **1**−**4** represent the first griseofulvin enantiomers with four absolute configurations (2*S*, 6'*S*; 2*R*, 6'*R*; 2*S*, 6'*R*; 2*R*, 6'*S*), and compounds **9**−**12** represent the first successful production of brominated griseofulvin derivatives from fungi via the addition of NaBr to the culture medium. In the antifungal assays, compounds **6** and **9** demonstrated significant inhibitory activities against the fungi *Colletotrichum truncatum*, *Microsporum gypseum*, and *Trichophyton mentagrophyte* with inhibition zones varying between 28 and 41 mm (10 μg/disc). The structure−activity relationship (SAR) was analyzed, which showed that substituents at C-6, C-7, C-6' and the positions of the carbonyl and double bond of griseofulvin derivatives significantly affected the antifungal activity.

Keywords Mangrove endophytic fungus · *Nigrospora* sp. · Griseofulvin · Antifungal activity

Introduction

Griseofulvin, a spirocyclic benzofuran-3-one fungal metabolite, was first isolated from *Penicillium griseofulvum* in 1939 by Oxford et al. (Oxford et al. 1939), used clinically for the treatment of tinea capitis and other superficial mycoses as a classic antifungal agent (Gentles et al. 1958; Williams et al. 1958). Tinea capitis was a common dermatophyte infection caused predominantly by *Trichophyton* or *Microsporum* species and the clinical presentations were seborrheic-like scale, 'black dot' pattern, inflammatory tinea capitis with kerion, and tiny pustules in the scalp (Gupta et al. 2000; Seebacher et al. 2007). Griseofulvin was the only drug available for treatment of tinea capitis before the approval of Terbinafine by the US Food and Drug Administration in 2007 (Rønnest et al. 2012).

In addition to antifungal effects, various other biological activities of griseofulvin were reported, including antitumor, anti-HIV, and marinated shrimp lethality (Rønnest et al.

Edited by Chengchao Chen.

✉ Bing Sun
sunb33@mail.sysu.edu.cn

✉ Bo Wang
ceswb@mail.sysu.edu.cn

✉ Zhigang She
cesshzhg@mail.sysu.edu.cn

[1] School of Chemistry, Sun Yat-sen University, Guangzhou 510275, China

[2] State Key Laboratory of Applied Microbiology Southern China, Guangdong Provincial Key Laboratory of Microbial Culture Collection and Application, Institute of Microbiology, Guangdong Academy of Sciences, Guangzhou 510070, China

[3] School of Pharmacy, Anhui Medical University, Hefei 230032, China

[4] Department of Chemistry, Women University Swabi, Swabi 23430, Pakistan

2009; Panda et al. 2005; Wei et al. 2016; Zhang et al. 2017). More than 400 griseofulvin analogues have been synthesized for drug screening since 1950 (Rønnest et al. 2009, 2012), but fewer than 20 new natural products of griseofulvin were reported in recent decades. Furthermore, the absolute configuration of most natural griseofulvin analogues was identified as 2*S*, 6'*R*, except for 6'-hydroxygriseofulvin (2*S*, 6'*S*) and leptosphaerin C (2*S*, 2'*S*, 6'*S*) (Lin et al. 2010; Shang et al. 2012).

Marine microorganisms have been considered as potential sources of structurally novel and biologically active secondary metabolites for drug discovery (Hai et al. 2021; Xu et al. 2022). The expressions of marine microorganism biosynthetic gene clusters, which are often silent under experimental laboratory culture conditions, impose restrictions on the discovery of new cryptic natural products. The addition of NaBr or other halogens to the culture medium, an important strategy of the OSMAC approach, may trigger fungal biosynthetic pathways to restore osmotic imbalances, which could activate different silent gene clusters for the discovery of new metabolites (Pan et al. 2019; Pinedo-Rivilla et al. 2022). For example, adding KBr to the rice medium led to the isolation of the brominated metabolite 2-bromogentisylalcohol from cultures of *Penicillium concentricum* (Ali et al. 2017) and adding NaBr to the rice medium led to the isolation of two new brominated azaphilones, bromophilones A and B from *Penicillium canescens* 4.14.6a (Frank et al. 2019). It is worth noting that four griseofulvin derivatives were reported from the two strains, but no brominated griseofulvin analogue was obtained after adding KBr or NaBr to the rice medium. In our group's previous research, one brominated cytochalasin, phomopchalasins E, and two iodized cytochalasin, phomopchalasins F and H, were isolated from *Phomopsis* sp. QYM-13 by adding NaBr or KI to the potato liquid medium, respectively (Chen et al. 2022).

Inspired by this approach, NaCl or NaBr was added to the rice solid medium of the mangrove-derived fungus *Nigrospora* sp. QQYB1 in an attempt to acquire halogen-substituted griseofulvin derivatives. Subsequently, LC–MS analysis of two extracts revealed the production of different halogen-substituted griseofulvin derivatives (Supplementary Fig. S56). The follow-up fermentation led to the isolation of four pairs of griseofulvin enantiomers (**1**–**4**) and 12 griseofulvin derivatives (**5**–**16**) (Fig. 1), including four bromide derivatives (**9**–**12**). Compounds **1**–**4** represented the first griseofulvin enantiomers with four absolute configurations (2*S*, 6'*S*; 2*R*, 6'*R*; 2*S*, 6'*R*; 2*R*, 6'*S*), and compounds **9**–**12** were the first successful production of brominated griseofulvin derivatives. Herein, we report the details of isolation, structure elucidation, antifungal and

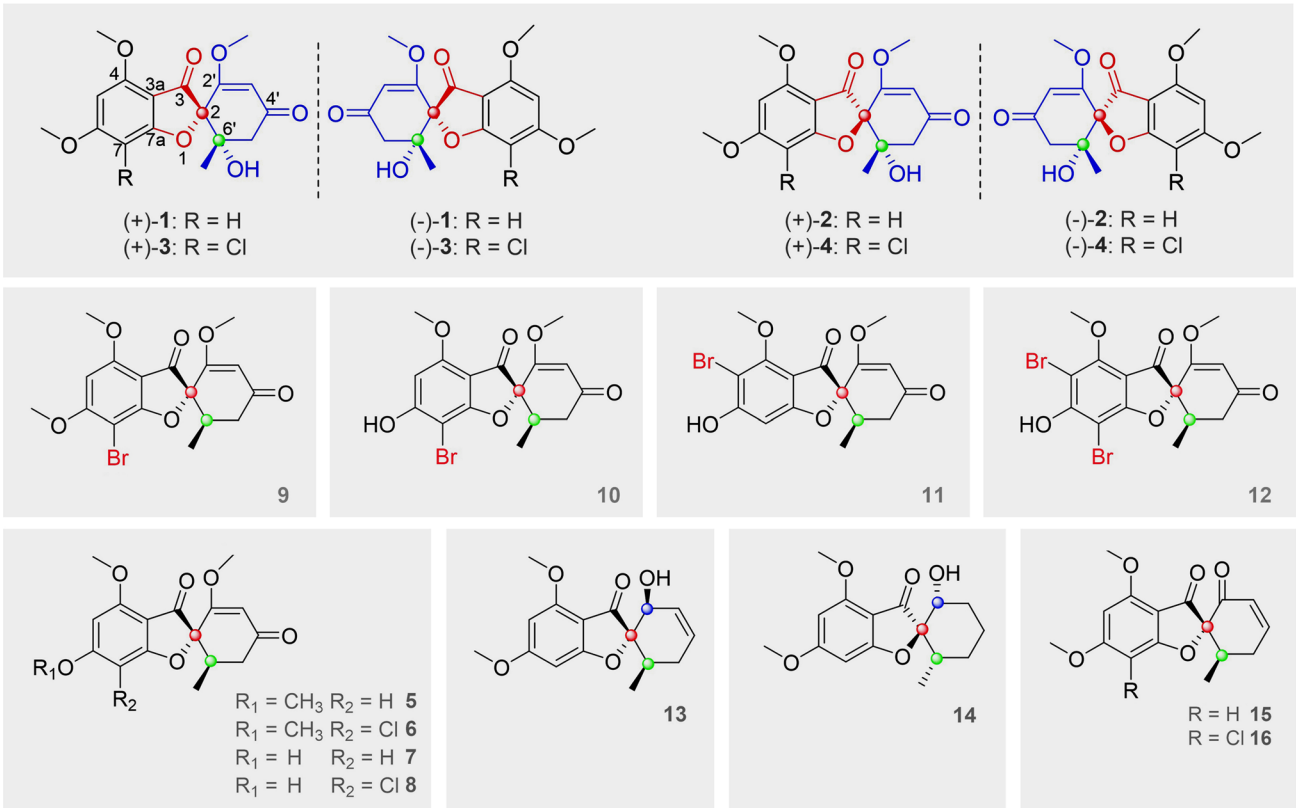

Fig. 1 Structures of griseofulvin derivatives **1**–**16**

antitumor activities, and the structure–activity relationship (SAR) of these metabolites.

Materials and methods

General experimental procedure

Optical rotations were measured on an MCP 300 (Anton Paar, Shanghai, China). UV spectra were performed in MeOH using a Shimadzu UV-2600 spectrophotometer (Shimadzu, Kyoto, Japan). ECD data were measured on a J-810 spectropolarimeter (JASCO, Tokyo, Japan). IR spectra were performed on IR Affinity-1 spectrometer (Shimadzu, Kyoto, Japan). Melting points were recorded on a Fisher–Johns hot-stage apparatus. NMR spectra were tested on a Bruker Avance spectrometer (Bruker, Beijing, China) (compounds **3 – 4**: 600 MHz for ^{1}H and 150 MHz for ^{13}C, respectively; compounds **1 – 2**, **10 – 12**, and **14 – 15**: 400 MHz for ^{1}H and 100 MHz for ^{13}C). HR-ESI-MS spectra were obtained on a ThermoFisher LTQ-Orbitrap-LC–MS spectrometer (Palo Alto, CA, USA). LC–MS analysis was recorded on a Q-TOF manufactured by Waters and a Waters acquity UPLC BEH C18 column (1.7 μm, 2.1 mm × 100 mm) was used for analysis. Silica gel (200–300 mesh, Marine Chemical Factory, Qingdao, China) and sephadex LH-20 (Amersham Pharmacia, Piscataway, NJ, USA) were used for column chromatography (CC). Silica gel plates (Qingdao Huang Hai Chemical Group Co., G60, F-254) were used for thin-layer chromatography (TLC). Semi-preparative HPLC (Ultimate 3000 BioRS, Thermo Scientific, Germany) was conducted using a Daice Chiralcel AD-H column (5 μm, 4.6 mm × 250 mm, Daicel, Japan), a Chiral INA column (5 μm, 4.6 mm × 250 mm, Phenomenex, USA), and a Chiral ND column (5 μm, 4.6 mm × 250 mm, Phenomenex, USA) for chiral separation. Single-crystal data were performed on an Agilent Gemini Ultra diffractometer (Cu *Kα* radiation, Agilent, Santa Clara, CA, USA).

Fungal material

The fungus *Nigrospora* sp. QQYB1 was isolated from healthy leaves of *Kandelia candel*, which were collected in March 2019 from Huizhou East Mangrove National Nature Reserve in Guangdong Province, China. The strain was identified as a *Nigrospora* sp. (GenBank No. OQ380944) by a BLAST search, which showed 99% identity to the sequence of a *Nigrospora* sp. (GenBank No. MT123052.1). The strain was deposited in the School of Chemistry, Sun Yat-sen University.

Fermentation

The fungus *Nigrospora* sp. QQYB1 was fermented on potato dextrose agar (PDA) for 5 days. The mycelia of the strain were cultivated on potato dextrose broth (PDB) for 3 days to prepare the seed culture. Then, the culture was inoculated into solid cultured medium (sixty 1000 mL Erlenmeyer flasks, each containing 50 g of rice, and 50 mL of distilled water with 0.3% NaCl or 2% NaBr) for 30 days at 25 °C.

Extraction and isolation

After the fermentation (adding 0.3% NaCl), the cultures were extracted three times with MeOH to yield 23.6 g of residue. Then, the crude extract was eluted using gradient elution with petroleum ether/EtOAc from 9:1 to 0:10 (*v/v*) on silica gel CC to get six fractions (Fr. A–F). Fr. C was applied to Sephadex LH-20 CC (CH_2Cl_2/MeOH, *v/v*, 1:1) to give three fractions (Fr. C_1–C_3). Fr. C_1 was subjected to silica gel CC (petroleum ether/EtOAc, *v/v*, 8:2) to yield compound **16** (23.4 mg). Fr. D was applied to Sephadex LH-20 CC (CH_2Cl_2/MeOH, *v/v*, 1:1) to give three fractions (Fr. $D_1 - D_3$). Fr. D_1 was subjected to silica gel CC (CH_2Cl_2/MeOH, *v/v*, 200:1) to yield compound **5** (128 mg). Fr. E was subjected to silica gel CC (petroleum ether/EtOAc, *v/v*, 6:4) to afford three fractions (Fr. E_1–E_2). Fraction E_1 was applied to Sephadex LH-20 CC (CH_2Cl_2/MeOH, *v/v*, 1:1) to give compound **6** (639 mg). Fr. E_2 was applied to silica gel CC (CH_2Cl_2/MeOH, *v/v*, 200:1 to 100:1) to give compounds **7** (30.2 mg) and **8** (29.6 mg). Fr. F was subjected to silica gel CC (petroleum ether/EtOAc, *v/v*, 5:5) to afford three fractions (Fr. F_1–F_2). Fr. F_2 (23 mg) was separated by normal phase HPLC on a chiral column (AD-H) (flow rate: 1.0 mL/min; solvent: n-hexane–isopropanol = 7:3) to yield (−)-**4** (2.2 mg, t_R 10.0 min), (+)-**3** (1.9 mg, t_R 22.5 min) and additional fraction Fr. $F_{2.2}$ (10 mg, t_R 19.0 min). Fr. $F_{2.2}$ was accomplished over a chiral column (INA) (flow rate: 1.0 mL/min; solvent: n-hexane–isopropanol = 7:3) to yield (+)-**4** (2.8 mg, t_R 11.7 min) and (−)-**3** (3.4 mg, t_R 13.5 min).

After the fermentation (adding 2% NaBr), the cultures were extracted using the same methods as above. The residue (15.8 g) was subjected to silica gel CC (200–300 mesh silica) with petroleum ether/EtOAc (9:1 to 1:9) to afford six fractions (Fr. A–F). Fr. C was subjected to Sephadex LH-20 CC (CH_2Cl_2/MeOH, *v/v*, 1:1) to obtain compound **15** (32.6 mg). Fr. D was subjected to silica gel CC (petroleum ether/EtOAc, *v/v*, 7:3), affording compound **12** (8.5 mg) and additional fraction Fr. D_1, which was subjected to silica gel CC (CH_2Cl_2/MeOH, *v/v*, 200:1) to yield compound **11** (4.3 mg), compounds **13** (4.2 mg) and **14** (3.4 mg). Fr. E was subjected to silica gel CC (petroleum ether/EtOAc, *v/v*, 6:4 to 5:5) to afford three fractions (Fr. E_1–E_4). Fr. E_1 was subjected to Sephadex LH-20 CC (CH_2Cl_2/MeOH, *v/v*, 1:1)

to obtain compound **9** (24.3 mg). Fr. E2 was subjected to Sephadex LH-20 CC (CH_2Cl_2/MeOH, *v/v*, 1:1) to obtain compound **10** (42.5 mg). Fr. E_3 was subjected to silica gel CC (petroleum ether/EtOAc, *v/v*, 6:4 to 5:5) to obtain compound (±)-**2** (15.7 mg). The chiral HPLC separation of (±)-**2** was accomplished over a chiral column (INA) (flow rate: 1.0 mL/min; solvent: n-hexane–isopropanol = 8:2) to yield (−)-**2** (5.9 mg, t_R 12.5 min) and (+)-**2** (6.2 mg, t_R 16.0 min). Fr. E_4 was subjected to silica gel CC (CH_2Cl_2/MeOH, *v/v*, 100:1) to obtain compound (±)-**1** (18.2 mg). In the same way, (±)-**1** was also purified by HPLC on a chiral column (ND) (flow rate: 1.0 mL/min; solvent: n-hexane–isopropanol = 7:3) to obtain (−)-**1** (8.3 mg, t_R 17.0 min) and (+)-**1** (6.1 mg, t_R 21.2 min).

(±)-6'-Hydroxy-7-dechlorogriseofulvin (**1**): White powder; mp 183.8−184.5 °C; UV (MeOH) λ_{max} (log ε): 211 (1.34), 288 (1.19) nm; IR ν_{max} 3397, 2922, 2851, 1697, 1616, 1587, 1506, 1456, 1348, 1219, 1157, 1114, 1039 cm^{-1}; ^1H NMR (400 MHz, $CDCl_3$) data, Table 1; ^{13}C NMR (100 MHz, $CDCl_3$) data, Table 2; HRESIMS *m/z* 335.11221 $[M+H]^+$ (calcd. for $C_{17}H_{19}O_7$, 355.11253). (+)-**1**, $[\alpha]_D^{25}$ + 350 (*c* 0.1 MeOH); ECD (*c* = 0.21 mg/mL, MeOH) λ_{max} ($\Delta\varepsilon$) 220 (− 19.5), 235 (+ 12.9), 292 (+ 14.6). (−)-**1**, $[\alpha]_D^{25}$− 340 (*c* 0.1 MeOH); ECD (*c* = 0.22 mg/mL, MeOH) λ_{max} ($\Delta\varepsilon$) 221 218 (+ 26.4), 236 (− 17.4), 294 (− 19.6).

(±)-6'-Hydroxy-7-dechloroepigriseofulvin (**2**): White powder; mp 183.8−184.5 °C; UV (MeOH) λ_{max} (log ε): 212 (1.46), 287 (1.19) nm; IR ν_{max} 3397, 2922, 2851, 1697, 1616, 1587, 1506, 1456, 1348, 1219, 1157, 1114, 1039 cm^{-1}; ^1H NMR (400 MHz, $CDCl_3$) data, Table 1; ^{13}C NMR (100 MHz, $CDCl_3$) data, Table 2; HRESIMS *m/z* 335.11221 $[M+H]^+$ (calcd. for $C_{17}H_{19}O_7$, 355.11253). (+)-**2**, $[\alpha]_D^{25}$+ 306 (*c* 0.1 MeOH); ECD (*c* = 0.19 mg/mL, MeOH) λ_{max} ($\Delta\varepsilon$) 219 (− 34.9), 236 (+ 13.7), 296 (+ 12.6).

Table 1 ^1H NMR data of **1** − **4** in $CDCl_3$ (*J* in Hz)

No	**1**[a]	**2**[a]	**3**[b]	**4**[b]
5	6.07, d (1.7)	6.07, d (1.5)	6.16, s	6.15, s
7	6.30, d (1.7)	6.22, d (1.5)		
3'	5.56, s	5.59, s	5.57, s	5.59, s
5'	3.23, d (16.6)	2.82, d (16.4)	3.19,d (16.6)	2.89, d (16.4)
	2.57, d (16.6)	2.69, d (16.4)	2.62, d (16.6)	2.75, d (16.4)
4-OCH_3	3.90, s	3.94, s	3.99, s	4.00, s
6-OCH_3	3.90, s	3.90, s	4.04, s	4.03, s
2'-OCH_3	3.62, s	3.65, s	3.63, s	3.65, s
6'-CH_3	1.19, s	1.27, s	1.20, s	1.31, s

[a]^1H NMR tested with 400 MHz.

[b]^1H NMR tested with 600 MHz.

Table 2 ^{13}C NMR data of **1** − **4** in $CDCl_3$

No	**1**[a]	**2**[a]	**3**[b]	**4**[b]
2	92.3, C	88.1, C	93.0, C	89.4, C
3	190.8, C	194.6, C	190.8, C	194.2, C
3a	104.1, C	105.3, C	105.0, C	105.9, C
4	159.6, C	159.3, C	158.3, C	158.0, C
5	93.9, CH	93.9, CH	90.1, CH	89.9, CH
6	170.7, C	171.0, C	165.0, C	165.2, C
7	89.0, CH	89.1, CH	97.8, C	97.9, C
7a	175.9, C	175.9, C	169.3, C	169.3, C
2'	168.7, C	169.1, C	168.1, C	168.5, C
3'	104.0, CH	104.9, CH	104.2, CH	105.1, CH
4'	195.7, C	195.9, C	195.4, C	195.6, C
5'	46.1, CH_2	47.2, CH_2	46.1, CH_2	47.2, CH_2
6'	74.8, C	74.5, C	74.7, C	74.7, C
4-OCH_3	56.3, CH_3	56.4, CH_3	56.6, CH_3	56.6, CH_3
6-OCH_3	56.3, CH_3	56.4, CH_3	57.2, CH_3	57.2, CH_3
2'-OCH_3	56.8, CH_3	56.8, CH_3	56.9, CH_3	56.9, CH_3
6'-CH_3	23.3, CH_3	23.7, CH_3	23.3, CH_3	23.9, CH_3

[a]^{13}C NMR tested with 100 MHz.

[b]^{13}C NMR tested with 150 MHz.

(−)-**2**, $[\alpha]_D^{25}$− 310 (*c* 0.1 MeOH); ECD (*c* = 0.20 mg/mL, MeOH) λ_{max} ($\Delta\varepsilon$) 218 (+ 52.2), 236 (− 20.1), 297 (− 18.8).

(±)-6'-Hydroxygriseofulvin (**3**): White powder; mp 153.4 − 114.9 °C; UV (MeOH) λ_{max} (log ε): 210 (1.70), 292 (1.39) nm; IR ν_{max} 3373, 2951, 2926, 2851, 1714, 1653, 1614, 1589, 1456, 1350, 1219, 1139, 1101 cm^{-1}; ^1H NMR (600 MHz, $CDCl_3$) data, Table 1; ^{13}C NMR (150 MHz, $CDCl_3$) data, Table 2; HRESIMS *m/z* 369.07324 $[M+H]^+$ (calcd. for $C_{17}H_{18}ClO_7$, 369.07356). (+)-**3**, $[\alpha]_D^{25}$+ 286 (*c* 0.03 MeOH); ECD (*c* = 0.18 mg/mL, MeOH) λ_{max} ($\Delta\varepsilon$) 221 (− 28.2), 236 (+ 40.9), 297 (+ 24.5). (−)-**3**, $[\alpha]_D^{25}$− 270 (*c* 0.05 MeOH); ECD (*c* = 0.17 mg/mL, MeOH) λ_{max} ($\Delta\varepsilon$) 221 (+ 12.2), 234 (− 29.6), 296 (− 19.3).

(±)-6'-Hydroxyepigriseofulvin (**4**): White powder; mp 153.4−154.9 °C; UV (MeOH) λ_{max} (log ε): 213 (1.17), 291 (0.92) nm; IR ν_{max} 3373, 2951, 2926, 2851, 1714, 1653, 1614, 1589, 1456, 1350, 1219, 1139, 1101 cm^{-1}; ^1H NMR (600 MHz, $CDCl_3$) data, Table 1; ^{13}C NMR (150 MHz, $CDCl_3$) data, Table 2; HRESIMS *m/z* 369.07324 $[M+H]^+$ (calcd. for $C_{17}H_{18}ClO_7$, 369.07356). (+)-**4**, $[\alpha]_D^{25}$+ 310 (*c* 0.1 MeOH); ECD (*c* = 0.19 mg/mL, MeOH) λ_{max} ($\Delta\varepsilon$) 220 (− 49.9), 238 (+ 38.2), 299 (+ 16.9). (−)-**4**, $[\alpha]_D^{25}$− 304 (*c* 0.1 MeOH); ECD (*c* = 0.20 mg/mL, MeOH) λ_{max} ($\Delta\varepsilon$) 220 (+ 49.5), 238 (− 38.3), 295 (− 15.4).

6-*O*-Desmethyl-7-bromogriseofulvin (**10**): White powder, mp 278.3−279.8 °C; $[\alpha]_D^{25}$ +298.9 (*c* 0.08 MeOH); UV (MeOH) λ_{max} (log ε): 213 (1.50), 238 (1.38), 292 (1.24) nm; ECD (*c* = 0.19 mg/mL, CD_3OD) λ_{max} ($\Delta\varepsilon$) 221 (− 51.7), 238 (+ 49.7), 295 (+ 17.1); IR ν_{max} 3331, 2964, 2922, 2852,

1697, 1603, 1408, 1359, 1223, 1130, 1018 cm^{-1}; ^1H NMR (400 MHz, MeOH) data, Table 3; ^{13}C NMR (100 MHz, CD_3OD) data, Table 4; HRESIMS *m/z* 383.01215 $[M+H]^+$ (calcd. for $C_{16}H_{16}BrO_6$, 383.01248).

5-Bromo-6-*O*-desmethyl-7-dechlorogriseofulvin (**11**): White powder, mp 264.8–266.2 °C; $[\alpha]_D^{25}$+ 298,5 (*c* 0.06 MeOH); UV (MeOH) λ_{max} (log ε): 218 (1.35), 240 (1.22), 285 (0.82) nm; ECD (*c* = 0.19 mg/mL, MeOH) λ_{max} ($\Delta\varepsilon$) 221 (−29.8), 245 (+33.7), 325 (+14.6); IR ν_{max} 3304, 2964, 2926, 2849, 1697, 1605, 1573, 1355, 1226, 1093 cm^{-1}; ^1H NMR (400 MHz, CD_3OD) data, Table 3; ^{13}C NMR (100 MHz, CD_3OD) data, Table 4; HRESIMS *m/z* 383.01221 $[M+H]^+$ (calcd. for $C_{16}H_{16}BrO_6$, 383.01248).

5,7-Dibromo-6-*O*-desmethylgriseofulvin (**12**): Colorless oil, $[\alpha]_D^{25}$+ 269.8 (*c* 0.08 MeOH); UV (MeOH) λ_{max} (log ε): 224 (1.32), 242, (1.23), 340 (0.84) nm; ECD (*c* = 0.18 mg/mL, CD_3OD) λ_{max} ($\Delta\varepsilon$) 218 (−19.3), 249 (+24.9), 329 (+11.4); IR ν_{max} 3373, 2941, 2849, 1647, 1595, 1456, 1360, 1231, 1180, 1055 cm^{-1}; ^1H NMR (400 MHz, MeOH) data, Table 3; ^{13}C NMR (100 MHz, CD_3OD) data, Table 4; HRESIMS *m/z* 460.92255 $[M+H]^+$ (calcd. for $C_{16}H_{15}Br_2O_6$, 460.92299).

3',4'-Dihydroeupenigriseofulvin (**14**): White powder, mp 217.4 – 218.5 °C; $[\alpha]_D^{25}$− 36.9 (*c* 0.08 MeOH); UV (MeOH) λ_{max} (log ε): 211 (1.66), 282 (1.05) nm; ECD (*c* = 0.17 mg/mL, MeOH) λ_{max} ($\Delta\varepsilon$) 214 (+17.6), 248 (−5.24), 286 (+3.04); IR ν_{max} 3428, 2959, 2926, 2859, 1659, 1616, 1585, 1456, 1217, 1155, 1120 cm^{-1}; ^1H NMR (400 MHz, $CDCl_3$) data, Table 3; ^{13}C NMR (100 MHz, $CDCl_3$) data, Table 4; HRESIMS *m/z* 293.13800 $[M+H]^+$ (calcd. for $C_{16}H_{21}O_5$, 293.13835).

Table 4 ^{13}C NMR data of **10** – **12**, **14** – **15** (100 MHz)

No	**10**[a]	**11**[a]	**12**[a]	**14**[b]	**15**[b]
2	91.8, C	91.1, C	91.7, C	95.7, C	95.4, C
3	193.7, C	193.0, C	192.2, C	197.0, C	190.8, C
3a	105.2, C	107.2, C	106.4, C	106.3, C	104.2, C
4	159.9, C	157.7, C	156.4, C	158.5, C	159.2, C
5	94.6, CH	99.6, C	102.0, C	92.6, CH	93.6, CH
6	167.5, C	166.5, C	165.5, C	169.8, C	170.3, C
7	84.3, C	94.7, CH	88.7, C	88.3, CH	88.7, CH
7a	173.4, C	175.7, C	172.0, C	175.7, C	176.2, C
2'	173.9, C	174.1, C	173.9, C	75.1, CH	190.6, C
3'	105.2, CH	105.2, CH	105.3, CH	29.3, CH_2	126.7, CH
4'	199.7, C	199.8, C	199.7, C	23.4, CH_2	152.5, CH
5'	40.8, CH_2	40.8, CH_2	40.8, CH_2	28.5, CH_2	31.4, CH_2
6'	37.5, CH	37.6, CH	37.6, CH	38.3, CH	37.3, CH
4-OCH_3	56.6, CH_3	62.7, CH_3	62.6, CH_3	55.6, CH_3	56.1, CH_3
6-OCH_3				55.6, CH_3	56.2, CH_3
2'-OCH_3	57.7, CH_3	57.6, CH_3	57.7, CH_3		
6'-CH_3	14.4, CH_3	14.5, CH_3	14.5, CH_3	15.6, CH_3	14.7, CH_3

[a]Data were recorded in CD_3OD.

[b]Data were recorded in $CDCl_3$.

4'-Demethoxyl-7-dechloroisogriseofulvin (**15**): White powder, mp 191.3–192.7 °C; $[\alpha]_D^{25}$+ 326 (*c* 0.12 MeOH); UV (MeOH) λ_{max} (log ε): 212 (1.53), 287 (1.02) nm; ECD (*c* = 0.20 mg/mL, MeOH) λ_{max} ($\Delta\varepsilon$) 235 (+44.3), 224 (−39.6), 314 (+25.3); IR ν_{max} 2960, 2922, 2851, 1697, 1683, 1616, 1591, 1506, 1456, 1215, 1157, 1120 cm^{-1}; ^1H NMR (400 MHz, $CDCl_3$) data, Table 3; ^{13}C NMR

Table 3 ^1H NMR data of **10** – **12**, **14** – **15** (400 MHz, *J* in Hz)

No	**10**[a]	**11**[a]	**12**[a]	**14**[b]	**15**[b]
5	6.21, s			5.96, d (1.7)	5.99, d (2.0)
7		6.41, s		6.16, d (1.7)	6.28, d (2.0)
2'				3.90, dd (11.8, 4.8)	
3'	5.62, s	5.62, s	5.64, s	2.30, m	6.08, dd (10.1, 2.1)
				1.86, m	
4'				1.83, m	7.14, ddd (10.1, 5.8, 2.2)
				1.39, m	
5'	2.90, dd (15.4, 13.2)	2.89, dd (16.4, 13.4)	2.90, dd (15.4, 13.2)	2.00, m	3.03, ddt (19.2, 11.0, 2.6)
	2.42, dd (15.4, 3.5)	2.42, dd (16.4, 4.4)	2.43, dd (15.5, 3.2)	1.50, m	2.47, dt (19.3, 5.7)
6'	2.83, m	2.78, m	2.85, m	1.92, m	2.75, m
4-OCH_3	3.87, s	4.05, s	4.02, s	3.86, s	3.85, s
6-OCH_3				3.85, s	3.87, s
2'-OCH_3	3.70, s	3.70, s	3.71, s		
6'-CH_3	0.91, d (6.4)	0.93, d (6.5)	0.93, d (6.2)	0.81, d (6.4)	1.01, d (6.7)

[a]Data were recorded in CD_3OD.

[b]Data were recorded in $CDCl_3$.

(100 MHz, $CDCl_3$) data, Table 4; HRESIMS *m/z* 289.10687 $[M+H]^+$ (calcd. for $C_{16}H_{17}O_5$, 289.10705).

X-ray crystallographic data

Colorless crystals of compounds (+)-**1**, **10**, **13**, **15** were obtained from n-hexane – EtOAc at room temperature by slow evaporation and measured on an Agilent Xcalibur Nova single-crystal diffractometer with Cu *Kα* radiation.

Crystal data of (+)-**1**: $C_{17}H_{18}O_7$, Mr = 334.31, tetragonal, $a = 8.76640(10)$ Å, $b = 8.76640(10)$ Å, $c = 19.7986(2)$ Å, $\alpha = 90°$, $\beta = 90°$, $\gamma = 90°$, $V = 1521.52(4)$ Å^3, $T = 100$ K, space group $P4_1$, Z = 4, μ(Cu *Kα*) = 0.964 mm^{-1}, 11,684 reflections collected, 3039 independent reflections ($R_{int} = 0.0225$, $R_{sigma} = 0.0170$). The final R_1 values were 0.0241, $wR2 = 0.0622$ [$I \geq 2\sigma(I)$]. The final R_1 values were 0.0243, $wR2 = 0.0623$ (all data). The goodness of fit on F^2 was 1.077. The flack parameter was 0.05(4). CCDC number: 2240676.

Crystal data of **10**: $C_{16}H_{15}BrO_6$, Mr = 383.20, orthorhombic, $a = 11.22120(10)$ Å, $b = 11.38150(10)$ Å, $c = 12.33490(10)$ Å, $\alpha = 90°$, $\beta = 90°$, $\gamma = 90°$, $V = 1575.34(2)$ Å^3, $T = 100$ K, space group $P2_12_12_1$, Z = 4, μ(Cu *Kα*) = 3.827 mm^{-1}, 15,338 reflections collected, 3153 independent reflections ($R_{int} = 0.0207$, $R_{sigma} = 0.0133$). The final R_1 values were 0.0185, $wR2 = 0.0494$ [$I \geq 2\sigma(I)$]. The final R_1 values were 0.0186, $wR2 = 0.0495$ (all data). The goodness of fit on F^2 was 1.052. The flack parameter was 0.011 (11). CCDC number: 2240679.

Crystal data of **13**: $C_{16}H_{18}O_5$, Mr = 290.30, monoclinic, $a = 6.02584(5)$ Å, $b = 10.47414(10)$ Å, $c = 11.75725(9)$ Å, $\alpha = 90°$, $\beta = 103.3219(8)°$, $\gamma = 90°$, $V = 722.096(11)$ Å^3, $T = 100$ K, space group $P2_1$, Z = 2, μ(Cu *Kα*) = 0.823 mm^{-1}, 13,155 reflections collected, 2734 independent reflections ($R_{int} = 0.0205$, $R_{sigma} = 0.0129$). The final R_1 values were 0.0264, $wR2 = 0.0693$ [$I \geq 2\sigma(I)$]. The final R_1 values were 0.0265, $wR2 = 0.0693$ (all data). The goodness of fit on F^2 was 1.104. The flack parameter was – 0.07(4). CCDC number: 2240681.

Crystal data of **15**: $(C_{16}H_{16}O_6)_2$, Mr = $(288.29)_2$, orthorhombic, $a = 9.59580(10)$ Å, $b = 11.28320(10)$ Å, $c = 25.9281(2)$ Å, $\alpha = 90°$, $\beta = 90°$, $\gamma = 90°$, $V = 2807.27(4)$ Å^3, $T = 100$ K, space group $P2_12_12_1$, Z = 4, μ(Cu *Kα*) = 0.846 mm^{-1}, 27,716 reflections collected, 5658 independent reflections ($R_{int} = 0.0384$, $R_{sigma} = 0.0238$). The final R_1 values were 0.0244, $wR2 = 0.0622$ [$I \geq 2\sigma(I)$]. The final R_1 values were 0.0251, $wR2 = 0.0625$ (all data). The goodness of fit on F^2 was 1.040. The flack parameter was – 0.01(4). CCDC number: 2240682.

LC–MS analysis

The LC–MS fingerprints of extracts were recorded with gradient elution using Bruker times TOF. The gradient was kept for 1 min at 10% MeOH–H_2O, then changed from 10% MeOH–H_2O to 40% MeOH–H_2O in 2 min, then 40% MeOH–H_2O was changed to 100% MeOH in 12 min, was maintained at 100% MeOH for the next 3 min, and then, 100% MeOH was transformed into 10% MeOH–H_2O within 0.1 min and maintained for 1.9 min. The elution rate was kept at 0.3 mL/min. The detection wavelength was 190–400 nm. The test samples are as follows: (A) *Nigrospora* sp. QQYB1, cultured with 0.3% NaCl in the medium; (B) *Nigrospora* sp. QQYB1, cultured with 2% NaBr in the medium.

ECD calculations, ^{1}H, ^{13}C NMR calculations, and DP4 + analysis

^{1}H, ^{13}C NMR calculations and ECD calculations were optimized with the Spartan'14 and Gaussian 09 software programs (Supplementary Tables S1–S6). The conformers with a Boltzmann population greater than 1% were selected for optimization at B3LYP/6–31 + G (d, p) and calculation at mPW1PW91-SCRF/6–311 + g (2d,p) (^{1}H and ^{13}C NMR) and B3LYP/6–31 + G (d, p) (ECD) (Frisch et al. 2009; Zhang et al. 2017). All calculations were carried out by the high-performance grid computing platform of Sun Yat-Sen University. The ECD spectra and DP4 + analysis were performed as described previously (Cui et al. 2018; Yang et al. 2021).

Antifungal assay

The disc diffusion assays of compounds **1**–**16** were measured against seven fungi, including *C. truncatum*, *P. expansum*, *A. flavus*, *A. niger*, *M. gypseum*, *T. mentagrophytes*, and *C. albicans* (Dahiya et al. 2016; Wang et al. 2018; Fang et al. 2022). Briefly, compounds **1**–**16** were dissolved in DMSO to final concentrations of 0.1–1 mg/mL. The spores of seven indicator fungi were resuspended in normal saline (0.91% *w/v* of NaCl) at a concentration of ~1×10^6 colonies mL^{-1} and spread on Sabouraud's dextrose agar plates. Then, the 6 mm paper discs saturated with 10 µL of compounds were placed on the petri plates. These plates were incubated for 48 h at 28 °C. After incubation, the presence/absence of fungal growth was observed, and the average diameter of the inhibition zone was calculated from triplicate sets. The results are given in Fig. 6 and Supplementary Table S7. Methanol and ketoconazole were used as negative and positive controls, respectively.

Cytotoxicity assay

The cytotoxicity of all compounds against HeLa (cervical), HepG2 (hepatocellular carcinoma), HCT-116 (human colorectal adenocarcinoma), and MCF-7 (breast cancer) human cancer cell lines were assessed using the MTT assay as previously described (Chen et al. 2016). Cisplatin was taken as the positive control.

Results and discussion

The strain *Nigrospora* sp. QQYB1 was isolated from the healthy leaves of *Kandelia candel*, collected from Huizhou East Mangrove National Nature Reserve in Guangdong Province, China. A further chemical investigation of *Nigrospora* sp. QQYB1, treated with 0.3% NaCl or 2% NaBr in rice solid medium, was carried out and led to isolation and identification of four pairs of griseofulvin enantiomers (**1–4**) and 12 griseofulvin derivatives (**5–16**), including four bromide derivatives (**9–12**). Compounds [(±)-**1–2**, (+)-**3**, (±)-**4**, **10–12, 14–15**] were determined as new griseofulvin derivatives by extensive spectroscopic analysis (1D and 2D NMR, HRESIMS), ECD spectra, computational calculation, DP4 + analysis, and X-ray single-crystal diffraction.

Compound (±)-**1** was obtained as white amorphous powder. Its molecular formula was assigned as $C_{17}H_{18}O_7$ on the basis of HRESIMS analysis (Supplementary Fig. S6) at *m/z* 335.11221 $[M+H]^+$ (calcd. for $C_{17}H_{19}O_7$, 335.11253), which was determined to possess 9 degrees of unsaturation. The ^{1}H NMR data (Supplementary Fig. S1; Table 1) of (±)-**1** showed two aromatic protons at δ_H 6.30 (1H, d, J = 1.7 Hz, H-7) and 6.07 (1H, d, J = 1.7 Hz, H-5), one olefinic proton at δ_H 5.56 (1H, s, H-3'), one methylene proton at δ_H 3.23 (1H, d, J = 16.6 Hz, H_a-5') and 2.57 (1H, d, J = 16.6 Hz, H_b-5'), three methoxyls at δ_H 3.90 (3H, s, 4-OCH_3), 3.90 (3H, s, 6-OCH_3) and 3.62 (3H, s, 2'-OCH_3), and one methyl δ_H 1.19 (3H, s, 6'-CH_3). Subsequently, the ^{13}C NMR data (Supplementary Fig. S2; Table 2) showed the presence of 17 carbon signals, including nine non-protonated carbons (δ_C 195.7, 190.8, 175.9, 170.7, 168.7, 159.6, 104.1, 92.3, and 74.8), three methine carbons (δ_C 104.0, 93.9 and 89.0), one methylene carbon (δ_C 46.1), three methoxyl carbons (δ_C 56.8, 56.3, and 56.3), and one methyl carbon (δ_C 23.3). The ^{1}H and ^{13}C NMR spectra of (±)-**1** were similar to those of 7-dechlorogriseofluvin (**5**) (Park et al. 2005), except for the absence of the methine moiety (δ_H 3.75, δ_C 37.2) and the presence of a nonprotonated carbon (δ_C 74.8). Moreover, the chemical shifts of C-2, C-5' and 6'-CH_3 in (±)-**1** were moved downfield within a range of 1.6 to 9.1×10^{-6} with compound **5**, and the HMBC correlations (Fig. 2; Supplementary Fig. S5) from H-5' to C-2, C-3' and 6'-CH_3 and 6'-CH_3 to C-2, C-5' and C-6' (Fig. 2), suggesting that the hydroxyl group was substituted at C-6' and the planar structure of (±)-**1** was determined as 6'-hydroxy-7-dechlorogriseofulvin.

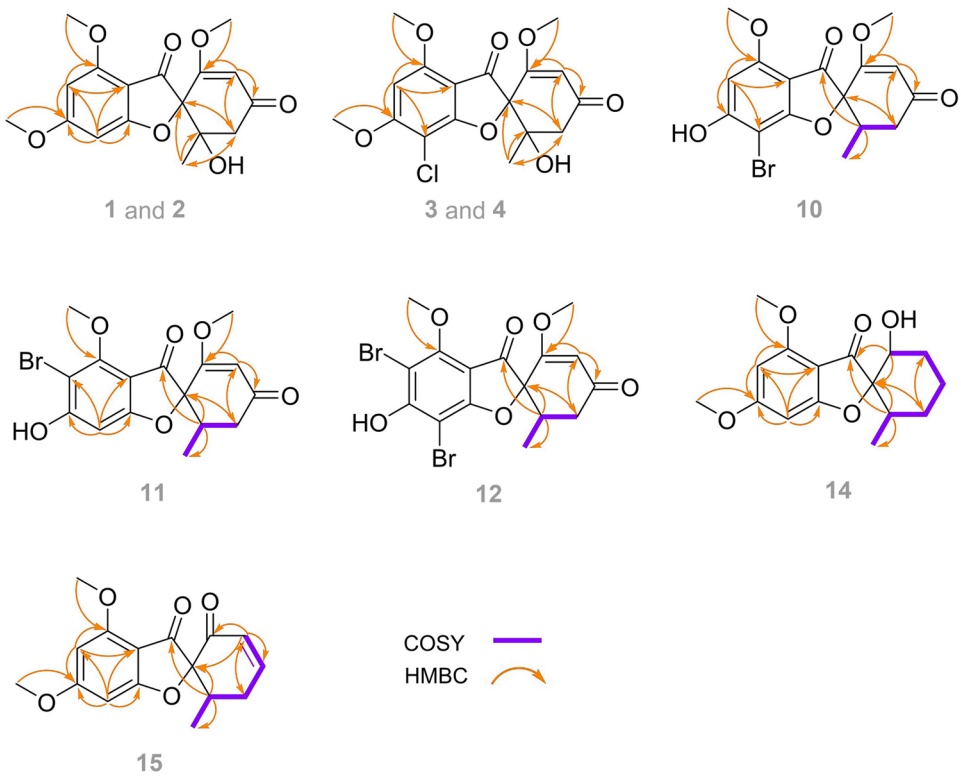

Fig. 2 Key COSY and HMBC correlations of **1–4**, **10–12**, and **14–15**

Subsequent chiral HPLC purification of (±)-**1** led to the separation of the two enantiomers (+)-**1** and (−)-**1** (Supplementary Fig. S57), which displayed opposite Cotton effects in their CD spectra and opposite optical rotations. The structure of (+)-**1** was subsequently confirmed by a single-crystal X-ray diffraction experiment using Cu *Kα* radiation [flack parameter 0.05(4)] (Fig. 3). Compared with experimental and calculated ECD curves (Fig. 4A), the absolute configurations of (+)-**1** and (−)-**1** were determined as 2*S*, 6'*S* and 2*R*, 6'*R*, respectively.

Compound (±)-**2** was isolated as a white amorphous powder, showing the same molecular formula as that of (+)-**1** (Supplementary Fig. S12). The ^{1}H and ^{13}C NMR spectra (Supplementary Figs. S7 and S8; Tables 1 and 2) of (±)-**2** were similar to those of (±)-**1**, except for the methylene proton at δ_H 3.23 (1H, d, J = 16.6 Hz, H_a-5'), 2.57 (1H, d, J = 16.6 Hz, H_b-5') in (+)-**1** was changed to δ_H 2.82 (1H, d, J = 16.4 Hz, H_a-5'), and 2.69 (1H, d, J = 16.4 Hz, H_b-5') in (±)-**2**. Comparing the same HMBC correlations (Fig. 2; Supplementary Fig. S11), compounds (±)-**2** and (±)-**1** were identified as epimers and compound (±)-**2** was named as 6'-hydroxy-7-dechloroepigriseofulvin. The separation of (±)-**2** on a chiral column was conducted to afford (+)-**2** and (−)-**2** (Supplementary Fig. S58). The absolute configurations of (+)-**2** and (−)-**2** were assigned as 2*R*, 6'*S* and 2*S*, 6'*R* by comparing the experimental and calculated ECD spectra (Fig. 4B).

Compound (±)-**3** was acquired as a white amorphous powder. The molecular formula was determined as $C_{17}H_{17}ClO_7$ based on the HRESIMS data (Supplementary Fig. S17). The ^{1}H and ^{13}C NMR spectra (Supplementary Figs. S13 and S14; Tables 1 and 2) of (±)-**3** were similar to those of (±)-**1** except the hydrogen atom in the C-7 was replaced by a chlorine atom. The relative configuration of (±)-**3** was determined as 2*S**, 6'*S** based on the similar chemical shifts at δ_H 3.19 (1H, d, J = 16.6 Hz, H_a-5'), 2.62 (1H, d, J = 16.6 Hz, H_b-5') in (±)-**3** and δ_H 3.23 (1H, d, J = 16.6 Hz, H_a-5'), and 2.57 (1H, d, J = 16.6 Hz, H_b-5') in (±)-**1**. The absolute configurations of (+)-**3** and (−)-**3** were determined as 2*S*, 6'*S* and 2*R*, 6'*R* by comparing the experimental ECD spectra (Fig. 4A) between (±)-**3** and (±)-**1**, respectively. In addition, (−)-6'-hydroxygriseofulvin was tentatively assigned as 2*S*, 6'*S* (Shang et al. 2012), but its ^{1}H and ^{13}C NMR spectra and optical rotation were consistent with those of (−)-**1** and (−)-**3**. Consequently, (−)-6'-hydroxygriseofulvin was further confirmed as 2*R*, 6'*R*.

Similarly, compound (±)-**4** showed the same molecular formula as that of (+)-**3** (Supplementary Fig. S22). Compounds (±)-**4** and (±)-**3** were identified as epimers according to the similar ^{1}H and ^{13}C NMR spectra of (±)-**4** with those of

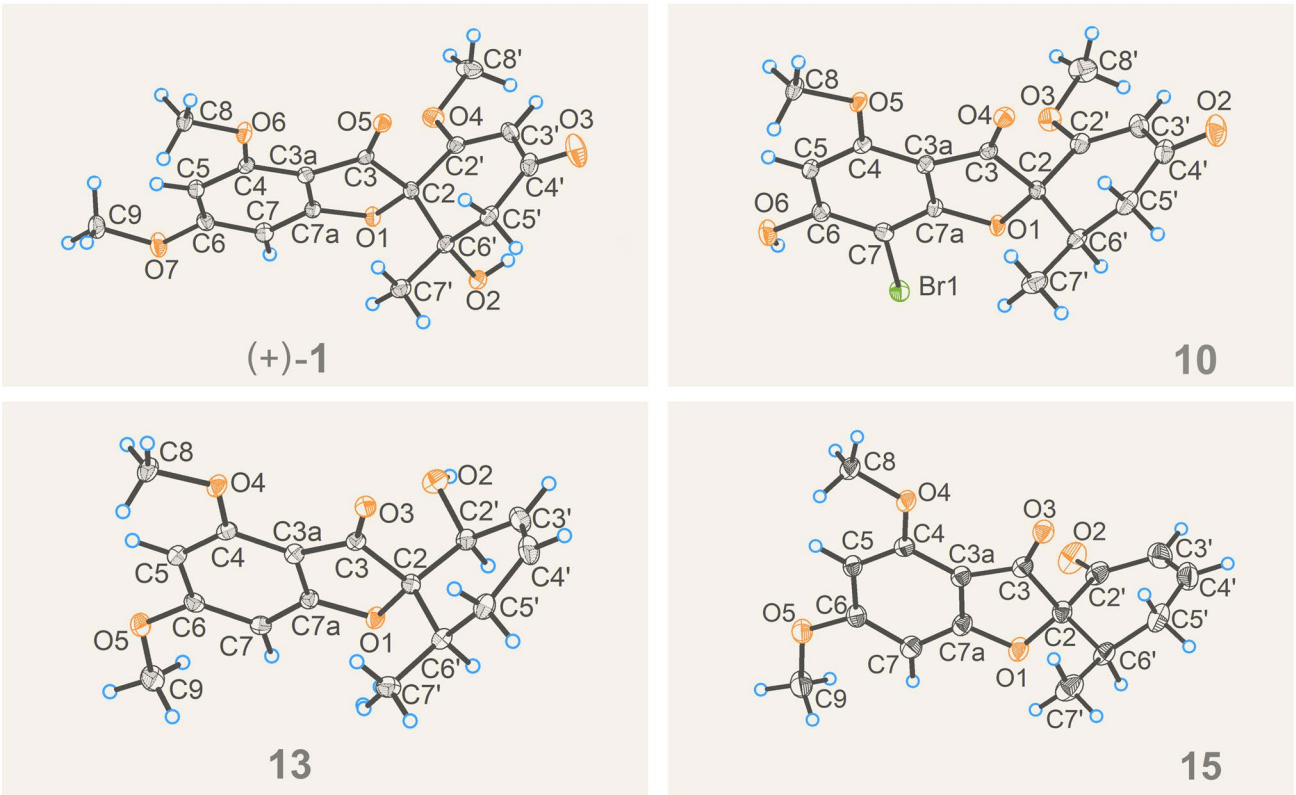

Fig. 3 Single-crystal X-ray structures of (+)-**1**, **10**, **13**, **15**

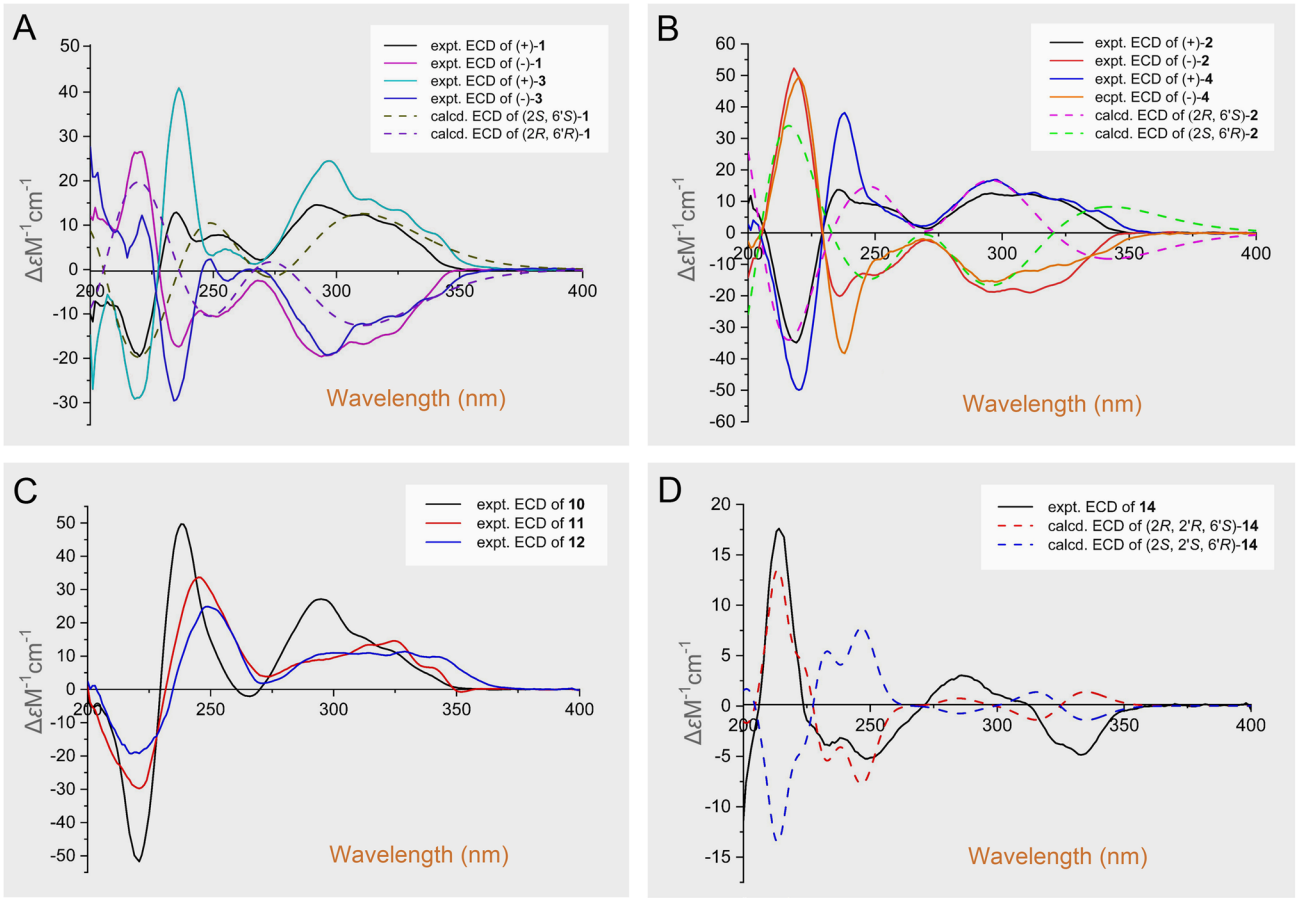

Fig. 4 A: Calculated ECD spectra of **1** and experimental ECD spectra of **1**, **3**; B: calculated ECD spectra of **2** and experimental ECD spectra of **2**, **4**; C: experimental ECD spectra of **10**–**12**; D: calculated and experimental ECD spectra of **14**

(±)-**3** (Supplementary Figs. S18 and S19; Tables 1 and 2), and the relative configuration of (±)-**4** was determined 2*S**, 6'*R** based on the similar chemical shifts at H-5 of (±)-**4** with that of (±)-**2**. The absolute configurations of (+)-**4** and (−)-**4** were assigned as 2*R*, 6'*S* and 2*S*, 6'*R* by the similar experimental ECD curves (Fig. 4B) of (±)-**4** and (±)-**2**.

Compound **10** was isolated as a white amorphous powder. The molecular formula was determined to be $C_{16}H_{15}BrO_6$ based on the HRESIMS data (Supplementary Fig. S28), and the bromine isotope pattern at *m/z* 383.01215 $[M+H]^+$ and 385.00977 $[M+2+H]^+$ (a ratio of 1:1) showed the presence of one bromine atom in the molecule. The ^1H and ^{13}C NMR spectra (Supplementary Figs. S23 and S24; Tables 3 and 4) of **10** were similar to those of 6-desmethylgriseofulvin (Belofsky et al. 1998). The difference between them was the chlorine atom at C-7 in **8** was replaced by a bromine atom in **10**. The absolute configuration of **10** was determined as 2*S*, 6'*R* by X-ray diffraction analysis [flack parameter 0.011(11)] (Fig. 3).

Compound **11** gave the same molecular formula as that of **10** based on the (+)-HRESIMS data (Supplementary Fig. S34). The ^1H and ^{13}C NMR data (Supplementary Figs. S29 and S30; Tables 3 and 4) suggested that **11** was structurally similar to **10**, and the main difference was the bromine atom was changed from C-7 to C-5, which was confirmed by the HMBC correlations (Fig. 2; Supplementary Fig. S33) from H-7 to C-3a, C-5, C-6, and C-7a. The coupling constant values of $^3J_{H\text{-}5',\,H\text{-}6'}$ (13.4 Hz, 4.4 Hz) of compound **11** were consistent to reported coupling constant values of $^3J_{H\text{-}5',\,H\text{-}6'}$ (13.2 Hz, 3.5 Hz) of compound **10**, and the relative configuration of **11** was determined as 2*S**, 6'*R** (Zhang et al. 2017). The absolute configuration of **11** was determined as 2*S*, 6'*R* by the similar experimental ECD curve (Fig. 4C) of **11** to that of **10**.

Compound **12** was isolated as a colorless oil. The molecular formula was determined as $C_{16}H_{14}Br_2O_6$ based on the HRESIMS data (Supplementary Fig. S40), and the bromine isotope pattern at *m/z* 460.92255 $[M+H]^+$, 462.92035 $[M+2+H]^+$, and 464.91833 $[M+4+H]^+$ (a ratio of 1:2:1) showed the presence of two bromine atoms in the molecule. The two-dimensional structure of **12** was similar to **10** by comparison of their NMR data (Supplementary Figs. S35

and S36; Tables 3 and 4). The distinction was the hydrogen atom in the C-5 was replaced by a bromine atom. The relative and absolute configurations were identical to **10** based on similar coupling constant values of $^{3}J_{\text{H-5', H-6'}}$ and ECD spectra (Fig. 4C).

Compound **14** was obtained as a white amorphous powder and had a molecular formula of $C_{16}H_{20}O_5$ based on the positive HRESIMS data (Supplementary Fig. S46). The ^{1}H and ^{13}C NMR data (Supplementary Figs. S41 and S42; Tables 3 and 4) suggested that **14** was structurally similar to **13** (Li et al. 2020). The main difference between them was the absence of two olefin protons in **13** and the presence of two methylene protons at δ_H 2.30 (1H, m, H_a-3') and 1.86 (1H, m, H_b-3'), 1.83 (1H, m, H_a-4'), and 1.39 (1H, m, H_b-4') in **14**, which was confirmed by the COSY correlations (Fig. 2; Supplementary Fig. S44) of H-2'/$H_{a,b}$-3'/$H_{a,b}$-4'/$H_{a,b}$-5'/H-6'/CH_3-6'. Thus, the planar structure of **14** was determined. To determine the stereostructure of C-2, C-2', and C-6', computational calculation and DP4 + probability were used to calculate the four possible relative configurations of **14**, and the relative configuration 2*S**, 2'*S**, 6'*R**-**14** matched with the experimental one (Supplementary Fig. S53 and S54). Comparing the experimental and calculated ECD spectra (Fig. 4D), **14** has the opposite rotation to **13**, and thus, the stereoconfiguration of **14** was assigned as 2*R*, 2'*R*, 6'*S*.

Compound **15** was purified as a white amorphous powder with a molecular formula of $C_{16}H_{16}O_5$ based on the HRESIMS data (Supplementary Fig. S52). The ^{1}H and ^{13}C NMR data (Supplementary Figs. S47 and S48; Tables 4 and 5) of **15** showed close resemblances to those of **16** (Levine et al. 1975), with the difference being the presence of one olefin proton (δ_H 6.28, d, J = 2.0 Hz, H-7). The HMBC correlations (Fig. 2; Supplementary Fig. S51) from H-7 to C-3a, C-5, C-6, and C-7a indicated that the chlorine atom at C-7 in **16** was replaced by a hydrogen atom in **15**. The relative and absolute configurations of **15** were clearly deduced under the guidance of single-crystal X-ray diffraction with Flack parameter − 0.01(4) (Fig. 3). Hence, the absolute configuration of **15** was determined as 2*S*, 6'*R*.

Seven known analogues were characterized as 7-dechlorogriseofulvin (**5**) (Park et al. 2005), griseofulvin (**6**) (Park et al. 2005), 6-*O*-desmethyl-7-dechlorogriseofulvin (**7**) (Shang et al. 2012), 6-*O*-desmethylgriseofulvin (**8**) (Belofsky et al. 1998), 7-bromogriseofulvin (**9**) (Schneck et al. 1968), eupenigriseofulvin (**13**) (Li et al. 2020), and 4'-demethoxylisogriseofulvin (**16**) (Levine et al. 1975) through comparison of the spectroscopic data with the literature data. Moreover, compounds **9** and **16** were reported as new natural products, and it was the first time the stereostructure of **13** was determined using the single-crystal X-ray diffraction experiment with a Flack parameter of − 0.07(4) (Fig. 3). In addition, (−)-6'-hydroxygriseofulvin was further confirmed as 2*R*, 6'*R* (Shang et al. 2012).

Eight dechlorogriseofulvin analogues [(±)-**1**−**2**, **5**, **7**, **14**−**15**] and four brominated griseofulvin derivatives (**9**−**12**) were obtained from *Nigrospora* sp. treated with 2% NaBr in rice solid medium. According to literature research, addition of NaBr or other halogens in the medium maybe triggers fungal biosynthetic pathways to restore osmotic imbalance, which could activate different silent gene clusters for the discovery of new metabolites (Pan et al. 2019; Pinedo-Rivilla et al. 2022). Moreover, the total biosynthetic pathway of griseofulvin (**6**) was mapped out (Fig. 5) (Cacho et al. 2013): griseophenone D underwent chlorination by the flavin-dependent halogenase *GsfI* to form griseophenone B and chloride ions were involved in the biological reaction directly. Similarly, compounds **9**−**12** were speculated to be formed from griseofulvin precursors through bromination with bromine ions.

Compounds **1**−**16** were tested for their antifungal activities against seven fungi, including four plant pathogenic fungi (*Colletotrichum truncatum*, *Penicillium expansum*, *Aspergillus flavus*, *Aspergillus niger*), two dermatophytes (*Microsporum gypseum*, *Trichophyton mentagrophytes*), and one deep infection yeast *Candida albicans* (Fig. 6; Supplementary Table S7). Compounds **6** and **9** demonstrated significant inhibitory activities against one plant pathogenic fungus (*C. truncatum*) and two dermatophytes (*M. gypseum*, *T. mentagrophyte*), with the inhibition zones varying between 28 and 41 mm (10 μg/disc), and showed weak or no antifungal activities against *P. expansum*, *A. flavus*, *A. niger*, and *C. albicans*. Other compounds exhibited weak or no inhibitory activity against these seven fungi with zones

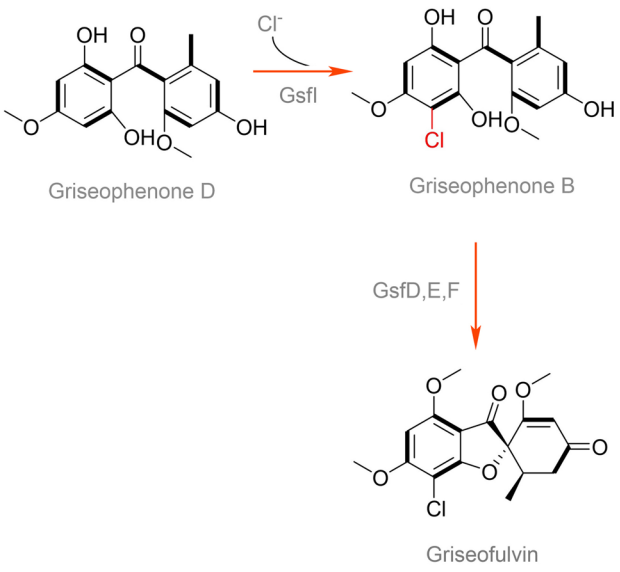

Fig. 5 Biosynthetic pathway of griseofulvin (**6**)

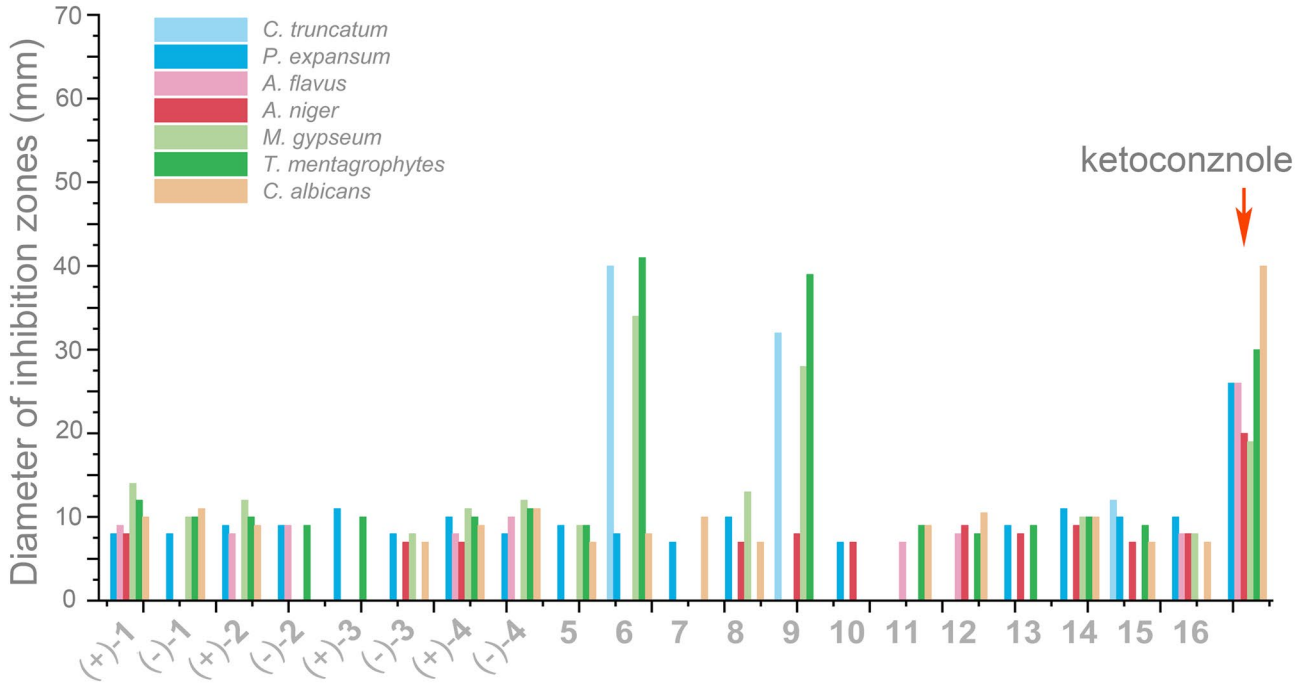

Fig. 6 Antifungal activities of compounds **1**–**16**

of inhibition ≤ 14 mm. According to the literature, griseofulvins were reported to exhibit in vitro fungistatic effects against dermatophytes, such as *Microsporum*, *Epidermophyton*, and *Trychophyton* genera, and the activities were restricted to yeast, actimomyces and *Nocardia* (Katrsev et al. 2019), which coincided with the experiments. The antifungal activity of griseofulvin against the plant pathogenic fungus *C. truncatum* has not been reported previously.

Comparing the activities of compounds **6**–**8** and **13**–**15** (or **9**–**12**), the methoxyl group at C-6 (R_1) improves the antifungal activity, and the antifungal activity was greatly reduced when R_1 was replaced by a hydroxyl group. Comparing the activities of compounds **5**–**6** and **9**, the halogen atom at C-7 (R_2) makes a contribution to antifungal activity; when the chlorine atom at C-7 was substituted by a bromine atom, the antifungal activity varied little. However, comparing the activities of compounds **1**–**4** and **6**, when R_3 was substituted with a hydroxyl, the activity decreased significantly. Comparing the activities of compounds **6** and **15**–**16**, the position of the carbonyl and double bond also have an important effect on activity. The SAR information mentioned above is generalized in Fig. 7.

In addition, all compounds were evaluated for their cytotoxicity against the HeLa (cervical), HepG2 (hepatocellular carcinoma), HCT-116 (human colorectal adenocarcinoma), and MCF-7 (breast cancer) human cancer cell lines. None of the compounds displayed cytotoxicity against any of the four cell lines at 50 μmol/L.

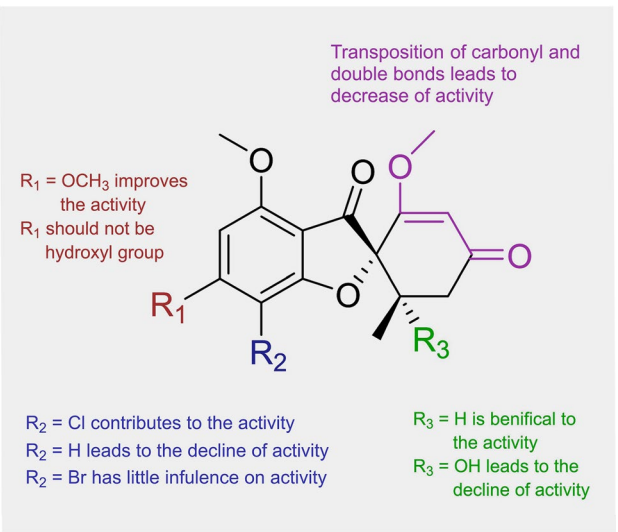

Fig. 7 SARs of griseofulvin derivatives on antifungal activities

Conclusions

In summary, processing of the mangrove-derived fungus *Nigrospora* sp. QQYB1, cultured with 0.3% NaCl or 2% NaBr in rice solid medium, led to the isolation of 12 new griseofulvin derivatives [(±)-**1**–**2**, (+)-**3**, (±)-**4**, **10**–**12**, **14**–**15**], two new natural products (**9** and **16**), and six

known analogues [(−)-**3**, **5**–**8**, and **13**]. Their 2D structures and absolute configurations were established by extensive spectroscopic analysis (1D and 2D NMR, HRESIMS), ECD spectra, computational calculation, DP4 + analysis, and X-ray single-crystal diffraction experiments. Compounds **1**–**4** represented the first natural griseofulvin enantiomers with four absolute configurations (2*S*, 6'*S*; 2*R*, 6'*R*; 2*S*, 6'*R*; 2*R*, 6'*S*), and compounds **9**– **12** were the first successfully produced brominated griseofulvin derivatives from fungi. Compounds **6** and **9** demonstrated significant inhibitory activity against one plant pathogenic fungus (*C. truncatum*) and two dermatophytes (*M. gypseum*, *T. mentagrophyte*) with inhibition zones ranging from 28 to 41 mm (10 μg/disc). The structure – activity relationship (SAR) indicated that the substituents at C-6, C-7, C-6' and the positions of the carbonyl and double bond were the main antifungal active sites of the griseofulvin derivatives.

Supplementary Information The online version contains supplementary material available at https://doi.org/10.1007/s42995-023-00210-0.

Acknowledgements This research was funded by the Guangdong Marine Economy Development Special Project (GDNRC[2022]35, GDNRC[2023]39) and the National Natural Science Foundation of China (U20A2001, 42276114).

Author contributions ZG performed the experiments and wrote the paper; LZ provided the pathogenic fungi; YW, CT, and LT participated in the experiments; LZ and CY analyzed the data and discussed the result; SG revised the manuscript; SB and WB reviewed the manuscript and SZ designed and supervised the experiments. All authors have read and agreed to the published version of the manuscript.

Data availability The data that support the findings of this study are included in this published article (and its supplementary information files).

Declarations

Conflict of interest The authors declare that they have no conflict of interest. Zhigang She is one of the Editorial Board Members, but he was not involved in the journal's review of, or decision related to, this manuscript.

Animal and human rights statement This article does not contain any studies with human participants or animals performed by the authors.

References

Ali T, Inagaki M, Chai HB, Wieboldt T, Rapplye C, Rakotondraibe LH (2017) Halogenated compounds from directed fermentation of *Penicillium concentricum*, an endophytic fungus of the liverwort *Trichocolea tomentella*. J Nat Prod 80:1397–1403

Belofsky GN, Gloer KB, Gloer JB, Wicklow DT, Dowd PF (1998) New p-terphenyl and polyketide metabolites from the sclerotia of *Penicillium raistrickii*. J Nat Prod 61:1115–1119

Cacho RA, Chooi YH, Zhou H, Tang Y (2013) Complexity generation in fungal polyketide biosynthesis: a spirocycle-forming P450 in the concise pathway to the antifungal drug griseofulvin. ACS Chem Biol 8:2322–2330

Chen SH, Chen DN, Cai RL, Cui H, Long YH, Lu YJ, Li CY, She ZG (2016) Cytotoxic and antibacterial preussomerins from the mangrove endophytic fungus *Lasiodiplodia theobromae* ZJ-HQ1. J Nat Prod 79:2397–2402

Chen Y, Yang WC, Zou G, Wang GS, Kang WY, Yuan J, She ZG (2022) Cytotoxic bromine- and iodine-containing cytochalasins produced by the mangrove endophytic fungus *Phomopsis* sp. QYM-13 using the OSMAC approach. J Nat Prod 85:1229–1238

Cui H, Liu YN, Li J, Huang XS, Yan T, Cao WH, Liu HJ, Long YH, She ZG (2018) Diaporindenes A-D: four unusual 2,3-dihydro-1*H*-indene analogues with anti-inflammatory activities from the mangrove endophytic fungus *Diaporthe* sp. SYSU-HQ3. J Org Chem 83:11804–11813

Dahiya R, Singh S, Sharma A, Chennupati SV, Maharaj S (2016) First total synthesis and biological screening of a proline-rich cyclopeptide from a caribbean marine sponge. Mar Drugs 14:228

Fang CY, Zhang QB, Zhang WJ, Zhang CS, Zhu YG (2022) Discovery of efrotomycin congeners and heterologous expression-based insights into the self-resistance mechanism. J Nat Prod 85:2865–2872

Frank M, Hartmann R, Plenker M, Mándi A, Kurtán T, Özkaya FC, Müller WEG, Kassack MU, Hamacher A, Lin WH, Liu Z, Proksch P (2019) Brominated azaphilones from the sponge-associated fungus *Penicillium canescens* strain 4.14.6a. J Nat Prod 82:2159–2166

Frisch MJ, Trucks GW, Schlegel HB, Scuseria GE, Robb MA, Cheeseman JR, Scalmani G, Barone V, Mennucci B, Petersson GA, Nakatsuji H, Caricato M, Li X, Hratchian HP, Izmaylov AF, Bloino J, Zheng G, Sonnenberg JL, Hada M, Ehara M et al (2009) Gaussian 09, Revision A.1. Gaussian Inc., Wallingford, CT

Gentles JC (1958) Experimental ringworm in guinea pigs: oral treatment with griseofulvin. Nature 182:476–477

Gupta AK, Summerbell RC (2000) Tinea capitis. Med Mycol 38:255–287

Hai Y, Wei MY, Wang CY, Gu YC, Shao CL (2021) The intriguing chemistry and biology of sulfur-containing natural products from marine microorganisms (1987–2020). Mar Life Sci Tech 3:488–518

Kartsev V, Geronikaki A, Petrou A, Lichitsky B, Kostic M (2019) Griseofulvin derivatives: synthesis, molecular docking and biological evaluation. Curr Top Med Chem 19:1145–1161

Levine SG, Hicks RE, Gottlieb HE, Wenkert E (1975) Carbon-13 nuclear magnetic resonance spectroscopy of naturally occurring substances. XXX Griseofulvin J Org Chem 40:2540–2542

Li YQ, Tan YH, Liu J, Zhou XF, Zeng SQ, Dong JD, Liu YH, Yang B (2020) A new griseofulvin derivative from a soft coral derived fungus *Eupenicillium* sp. SCSIO41208. Nat Prod Res 34:2971–2975

Lin J, Liu SC, Sun BD, Niu SB, Li EW, Liu XZ, Che YS (2010) Polyketides from the ascomycete fungus *Leptosphaeria* sp. J Nat Prod 73:905–910

Oxford AE, Raistrick H, Simonart P (1939) Studies in the biochemistry of micro-organisms: griseofulvin, $C_{17}H_{17}O_6Cl$, a metabolic product of *Penicillium griseofulvum* Dierckx. Biochem J 33:240–248

Pan R, Bai X, Chen JM, Zhang HW, Wang H (2019) Exploring structural diversity of microbe secondary metabolites using OSMAC strategy: a literature review. Front Microbiol 10:294

Panda D, Rathinasamy K, Santra MK, Wilson L (2005) Kinetic suppression of microtubule dynamic instability by griseofulvin: Implications for its possible use in the treatment of cancer. P Natl Acad Sci USA 102:9878–9883

Park JH, Choi GJ, Lee SW, Kim KM, Jung HS, Jang KS, Cho KY, Kim JC (2005) Griseofulvin from *Xylaria* sp. strain F0010, an

endophytic fungus of abies holophylla and its antifungal activity against plant pathogenic fungi. J Microbiol Biotechn 15:112–117
Pinedo-Rivilla C, Aleu J, Durán-Patrón R (2022) Cryptic metabolites from marine-derived microorganisms using OSMAC and epigenetic approaches. Mar Drugs 20:84
Rønnest MH, Rebacz B, Markworth L, Terp AH, Larsen TO, Krämer A, Clausen MH (2009) Synthesis and structure-activity relationship of griseofulvin analogues as inhibitors of centrosomal clustering in cancer cells. J Med Chem 52:3342–3347
Rønnest MH, Raab MS, Anderhub S, Boesen S, Krämer A, Larsen TO, Clausen MH (2012) Disparate SAR data of griseofulvin analogues for the dermatophytes *Trichophyton mentagrophytes*, *T. rubrum*, and MDA-MB-231 cancer cells. J Med Chem 55:652–660
Schneck DW, Racz WJ, Hirsch GH, Bubbar GL, Marks GS (1968) Studies of the relationship between chemical structure and porphyria-inducing activity—IV: Investigations in a cell culture system. Biochem Pharmacol 17:1385–1399
Seebacher C, Abeck D, Brasch J, Cornely O, Daeschlein G, Effendy I, Ginter-Hanselmayer G, Haake N, Hamm G, Hipler C, Hof H, Korting HC, Kramer A, Mayser P, Ruhnke M, Schlacke KH, Tietz HJ (2007) Tinea capitis: ringworm of the scalp. Mycoses 50:218–226
Shang Z, Li XM, Li CS, Wang BG (2012) Diverse secondary metabolites produced by marine-derived fungus *Nigrospora* sp. MA75 on various culture media. Chem Biodivers 9:1338–1348
Wang JF, Cong ZW, Huang XL, Hou CX, Chen WH, Tu ZC, Huang DY, Liu YH (2018) Soliseptide A, a cyclic hexapeptide possessing piperazic acid groups from *Streptomyces solisilvae* HNM30702. Org Lett 20:1371–1374
Wei MY, Xu RF, Du SY, Wang CY, Xu TY, Shao CL (2016) A new griseofulvin derivative from the marine-derived *Arthrinium* sp. fungus and its biological activity. Chem Nat Compd 52:1011–1014
Williams DI, Marten RH, Sarkany I (1958) Oral treatment of ringworm with griseofulvin. Lancet 2:1212–1213
Xu WF, Wu NN, Wu YW, Qi YX, Wei MY, Pineda LM, Ng MG, Spadafora C, Zheng JY, Lu L, Wang CY, Gu YC, Shao CL (2022) Structure modification, antialgal, antiplasmodial, and toxic evaluations of a series of new marine-derived 14-membered resorcylic acid lactone derivatives. Mar Life Sci Tech 4:88–97
Yang WC, Yuan J, Tan Q, Chen Y, Zhu YJ, Jiang HM, Zou G, Zang ZM, Wang B, She ZG (2021) Peniazaphilones A-I, produced by co-culturing of mangrove endophytic fungi, *Penicillium sclerotiorum* THSH-4 and *Penicillium sclerotiorum* ZJHJJ-18. Chin J Chem 39:3404–3412
Zhang DW, Zhao LL, Wang LN, Fang XM, Zhao JY, Wang XW, Li L, Liu HY, Wei YZ, You XF, Cen S, Yu LY (2017) Griseofulvin derivative and indole alkaloids from *Penicillium griseofulvum* CPCC 400528. J Nat Prod 80:371–376